RESEARCH STATUS ON THE ECRIPAC ACCELERATOR CONCEPT

A. Cernuschi*[1], T. Thuillier[1], L. Garrigues[2], A. Beck[3]
[1]Laboratoire de Physique Subatomique et de Cosmologie, Grenoble, France
[2]Laboratoire Plasma et Conversion d'Energie, Toulouse, France
[3]Laboratoire Leprince-Ringuet, Palaiseau, France

Abstract

This study presents the current advancement on our investigation of the Electron Cyclotron Resonance Ion Plasma Accelerator (ECRIPAC), revisiting and expanding this original accelerator concept initially developed in the ninties. ECRIPAC is an innovative compact plasma device able to generate energetic pulsed ion beams using robust and well mastered electron cyclotron resonance ion source technologies, without requirements for axial RF cavities or powerful laser beams. It relies on the gyromagnetic auto-resonance of plasma electrons in a time growing magnetic field, followed by the axial acceleration of ions through the plasma space-charge field inside a magnetic field gradient, up to energies close to 100 MeV/A. The theoretical behaviour of ECRIPAC is summarized. Some preliminary results of kinetic plasma simulations inside a preliminary design of an ECRIPAC machine able to accelerate He^{2+} ions up to ≈ 10 MeV/A are presented. Two sets of simulations are considered, one working with a cylindrical geometry and azimuthal mode decomposition in the open-source code Smilei and the other using a 3D geometry in the open-source code WarpX, providing interesting insights on the plasma behaviour inside the accelerator.

INTRODUCTION

The Electron Cyclotron Resonance Ion Plasma Accelerator (ECRIPAC) [1] is an original concept proposed by R. Geller, consisting in a plasma-based particle accelerator able to generate very energetic pulsed ion beams. Owing to its compact dimensions and the well-mastered technologies used in its design, the ECRIPAC is suitable for a wide array of applications, with a particular focus in the medical field as a possible instrument for ion cancer therapy. In our recent publications [2, 3], we reviewed and corrected the physical theory behind the ECRIPAC, and a short resume of its working principles and operating cycle is proposed in the the rest of this section.

An ECRIPAC device, which is schematically represented in Fig. 1, is composed of three main section. The first one is an injector of a highly ionized low-pressure plasma, with a possible candidate being an ECR ion source [4]. The second one is called the GYRAC section, which is characterized by the presence of a microwave injector and a reverse pulsed field coil acting on a small part of the accelerating cavity, generating a transient magnetic mirror trap which is slowly restored over time (red curve in Fig. 1). The third one is the PLEIADE section, composed by the rest of the accelerating

* cernuschi@lpsc.in2p3.fr

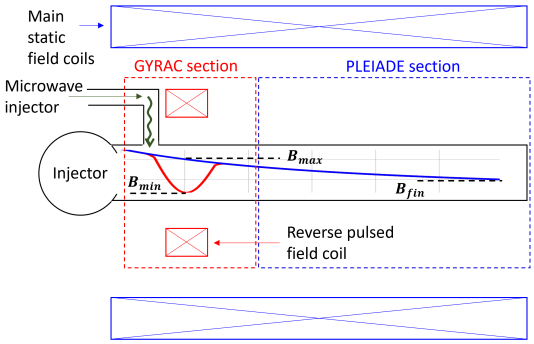

Figure 1: Schematic representation of an ECRIPAC device and the magnetic field generated inside the cavity. The blue curve represents the magnetic field profile when the pulsed coil is turned off (with $B_{\max}$ and B_{fin} being the maximum and final field intensities respectively), while the red curve is the magnetic field profile in the GYRAC section when the pulsed coil is working at its maximum power ($B_{\min}$ is the minimum field intensity inside the mirror trap).

cavity. Some static coils encompass the whole device, generating a static field represented with a blue curve in Fig. 1. The ECRIPAC working cycle is composed by three main phases: the gyromagnetic autoresonance (GA) phase, the plasma compression (PC) phase and the PLEIADE (PL) phase. The GA phase starts with the injection of both the plasma and the microwave when the pulsed coil reaches its maximum power, generating a magnetic mirror trap with an intensity equal to $B_{\min}$ at its center, which must be close to the magnetic field value satisfying the ECR condition for the injected microwave with frequency ω_{HF} ($B_{\text{ECR}} = m\omega_{\text{HF}}/e$ where m and e are the mass and the charge of the electron). The interaction of the plasma with the injected microwave inside a magnetic field growing over time onsets a physical phenomena called gyromagnetic autoresonance [5, 6] (GA), which determines a synchronous increase of the electron energy with the magnetic field

$$\gamma(t) = \frac{B(t)}{B_{\min}}\,, \tag{1}$$

where γ is the electron Lorentz factor. The PC phase starts when the microwave injection is halted, while the magnetic field is still increasing. During this phase, the plasma bunch is compressed under the action of the electric field induced by the variation of the magnetic field over time, which also further increases the electron energy. The plasma compression lasts until the restoration of the static field, which determines the start of the PL phase, where the ions are accelerated by the electrons through ion entrainment [7].

Indeed, the negative gradient of the static magnetic field along the axis determines the insurgence of a ∇B force able to displace the electron bunch from the ions, generating a space-charge field which accelerates the latter. Since the electrons and the ions have been experimentally observed to yield similar final velocities [7], the process results in a net conversion of the electron perpendicular energy $W_{e,\perp}$, which is accumulated during the GA and PC phases, in parallel ion energy $W_{i,\parallel}$

$$W_{e,\perp}^{in} - W_{e,\perp}^{fin} \approx W_{i,\parallel} \ , \tag{2}$$

where the indexes *in* and *fin* stand for the initial and final, and the $\perp$ and $\parallel$ directions are considered with respect to the cavity axis. The stability of the ion acceleration during the PL phase strongly depends on the magnetic field profile, which must respect several criteria. Our recent theoretical investigation of the accelerator stability [2] highlighted more stringent limitations than initially predicted, leading to the conclusion that the ECRIPAC is better suited to accelerate ions with small mass-over-charge ratio using a dense plasma, properly tuning the microwave and coils settings. Using these results, we developed several prototype designs for accelerators of interest in the medical field. A particular focus was devoted to a compact He^{2+} accelerator, able to accelerate ions up to almost 10 MeV/A inside a 1.8 m long cavity. The electron dynamics inside this prototype design has been validated using a Monte-Carlo particle-tracking code, and some theoretical estimations for the extracted beam parameters have been detailed. This work proposes some preliminary results of the kinetic plasma modeling inside the He^{2+} accelerator design using Particle-In-Cell (PIC) simulations, to better understand the plasma behavior inside the ECRIPAC during its operating cycle.

SIMULATION SETTINGS

The kinetic plasma modeling inside the He^{2+} accelerator design has been carried out using electromagnetic PIC simulations [8]. This choice is dictated by the requirement to properly resolve the short timescale characterizing gyromagnetic autoresonance, which depends on the relative phase between the injected microwave and the electron velocity during the electron cyclotron motion. The static and pulsed magnetic fields generated by the external coils, including the induced electric field, have been evaluated through bilinear interpolation at the nodes of field maps, characterized by a resolution of 250 µm. The static field map has been generated through the FEM software POISSON Superfish [9], while COMSOL Multiphysics [10] has been used for the pulsed field maps. The injected microwave has been implemented through an analytical formulation, considering either a transverse plane wave (PW) propagating in the system or a TE_{111} (transverse electric) mode excited inside the cavity. The initial magnetic mirror trap, corresponding to the magnetic field profile when the pulsed coil is operating at its maximum power, is characterized by a minimum value B_{min} and a mirror length equal to approximately 0.086 T and 40 cm respectively. When the static field is fully restored, the magnetic field profile is defined by B_{max} and B_{fin} values equals to 5 T and 4.89 T respectively. To complete the simulations in a reasonable time, we were forced to greatly increase the frequency of the pulsed coil f_{pul} (up to 200 kHz) with respect to the realistic value for the considered design (1-10 Hz). This approach has already been adopted in several numerical simulations of GYRAC devices [11–14], yielding successful comparisons with experimental setups working at a much lower pulsed coil frequency than the simulated one. The injected microwave oscillates at a frequency f_{HF} of 2.45 GHz, with a nominal intensity E_{HF} of 1 kV/cm. The spatial grid of the PIC simulation has a precision of approximately 200 µm, lower than the estimated Debye length, in order to properly resolve the Debye shielding inside the system. The temporal step for the time advancement corresponds to 0.95 of the Courant condition [8]. The boundaries of the system consists in a cavity with a 50 cm radius and a variable length depending on the simulation. Silver-Muller absorbing boundaries conditions [15] (BC) are applied at all boundaries for the electromagnetic fields, while removing BC [8] have been considered for all the particles inside the system. The plasma is composed by two populations, the electrons and the He^{2+} ions. A homogeneous neutral plasma with a cylindrical shape (radius and length equal to 10 mm) is generated at the start of the simulation, with an initial electron density of 1.11×10^{16} m^{-3}, equal to 15% of the critical density for a 2.45 GHz microwave. The electrons and ions are initialized with a rectangular distribution around an initial average temperature of 200 eV and 10 eV respectively, with no preferential direction for the initial velocity.

Two sets of simulations have been carried out. The first one (S1) employ a cylindrical geometry with azimuthal mode (AM) decomposition [16]. This technique allows simulating nearly cylindrically symmetric systems by solving Maxwell's equations with the electromagnetic fields expressed as a Fourier series in the angular direction. The computational cost of the simulation using AM decomposition is greatly reduced compared to the 3D case, while still maintaining the same physical results if the problem does not deviate too much from the cylindrical symmetry. S1 has been developed using the Smilei code [17], applying external field maps with AM decomposition. The typical simulation used 32 particle per cell (PPC), 2 in both the radial and axial direction and 8 in the azimuthal one. The second set of simulations (S2) consists in fully three dimensional simulations of the system, and has been carried out using the WarpX code [18], which has been noted to require a much lower computational cost for our problem. In this case, we used only 8 PPC (2 in each Cartesian direction) to complete the simulations in a reasonable time ($\approx$ 15 kCPUh for the GA phase) with a hybrid MPI/OpenMP parallelization on 512 CPUs.

SIMULATION RESULTS

Both S1 and S2 validate the proper working of the GA phase inside the considered accelerator design. The elec-

trons trapped in GA forms a bunch rotating around the cavity axis, with energies close to the predicted value (≈ 2 MeV at the end of the GA phase). The non-trapped electrons are instead confined close to the cavity axis. The ions initially expand to generate a ring-like structure with approximately the same radius as the rotating electron bunch, which slowly morphs into the shape of a disk with a distinct density peak in the center. The ion energy distribution function resembles a Maxwell-Boltzmann distribution, with most ions having energies in the order of few hundreds eV.

The lower computational cost of S1 allowed to investigate the effects of the magnetic field increase rate, determined by f_{pul}, and several other parameters on the system. The results of the S1 simulations are reported in Table 1. A clear trend arising from the results is that a higher f_{pul} yields a larger fraction of confined particles and trapped electrons in GA. Moreover, a lower f_{pul} value requires a longer cavity length L_{c} inside the simulation to improve the number of confined particles. This behavior is probably related to the slower dynamics of GA, requiring more time for the creation of the relativistic electron bunch. As a result, the longitudinal oscillations of the electrons inside the mirror trap play a more important role on the electron dynamics, and require a larger portion of the magnetic mirror to be simulated to avoid the premature electrons' deconfinement. The fraction of confined ions follows a similar trend to the electrons' one, due to the plasma tendency to restore the charge imbalance arising inside the system. The results are particularly discouraging for $f_{\mathrm{pul}} = 50$ kHz, for which even a 18 cm long cavity is not sufficient to avoid consistent particle losses. An even longer cavity is thus required for physical results, greatly increasing the computational cost of the simulation. Moreover, the limitations of the AM decomposition techniques are highlighted by the simulation with $f_{\mathrm{pul}} = 100$ kHz using three AM instead of two. Considerable improvements are observed with three AM in both the fraction of confined particles and trapped electrons, suggesting that several effects arising from important deviations from the cylindrical symmetry are not well captured in the simulations.

Preliminary simulations of the PC phase were also carried out using S1. $f_{\mathrm{pul}} = 200$ kHz has been found to determine an excessively fast compression of the plasma, leading to strong plasma instabilities and a subsequent deconfinement of approximately 50% of the initial plasma population. When f_{pul} is reduced to 100 kHz, the electrons follow a much more regular dynamics, with the relativistic electron bunch morphing into a ring-like structure as predicted by theory. Moreover, it has been noted that a gradual decrease of E_{HF} up to zero is required for an improved electron confinement. Unfortunately, AM decomposition does not provide meaningful insights on the ion dynamics. Indeed, the use of this technique together with external fields leads to the insurgence of numerical instabilities along the cavity axis, which grow over time. While they have negligible effects on the dynamics of trapped electrons, which do not populate the center of the cavity, the presence of a dense ion population nearby the axis leads to its interaction with the instabilities, leading to an nonphysical ions' accumulation in a specific point of the cavity.

Such instabilities are not present in S2, which highlights the necessity of a 3D PIC simulation despite the larger computational cost. The only results currently available are the more restrictive requirements on the magnetic field increase rate during GA when using a TE_{111} mode instead of PW to model the injected microwave. Indeed, the theoretical requirement to onset GA [5, 6] ($dB/dt < E_{\mathrm{HF}}\omega_{\mathrm{HF}}$) is sufficient when using the PW model, while a strong de-trapping of electrons from GA is observed when using the TE_{111} mode with the other simulation settings kept fixed. The same behavior has also been observed in S1, allowing some comparisons between the two sets of simulations. S1 and S2 show similar electron and ion spatial distributions and energy spectra, which allow us to consider physically reliable the insights gained from S1 during the GA phase.

Table 1: Results for S1 simulations. f_{pul}, L_{c}, n° AM, CE, TE, CI stand for pulsed coil frequency, cavity length, number of azimuthal modes, confined electrons, electrons trapped in GA and confined ions respectively.

f_{pul} [kHz]	L_{c} [cm]	n° AM	% CE	% TE	% CI
200	4	2	84.9	83.2	84.4
100	8	2	66.8	56.9	76.5
100	8	3	73.0	66.5	82.7
50	8	2	25.7	16.7	27.7
50	18	2	54.7	22.9	66.8

CONCLUSIONS

This work presents some preliminary results of kinetic plasma simulations inside a prototype design for a He^{2+} ECRIPAC device, which was presented in our previous publication [3]. A first set of PIC simulations employed the AM decomposition technique to work with a quasi-cylindrically symmetric system, strongly reducing the computational cost of the simulations. We found out that a larger increase rate of the magnetic field is beneficial for the GA phase, increasing the confinement of the plasma and the number of electron trapped in GA, while also requiring a shorter cavity length for the simulation. Nevertheless, an excessively fast compression during the PC phase generates plasma instabilities. The AM decomposition technique has been found to be unsuitable to fully simulate the ECRIPAC during the PC phase, and thus a second set of 3D PIC simulations is currently under development. Preliminary results show a more restrictive requirement than the theoretical one when using a TE_{111} mode to model the injected microwave, and comparable results with the previous set of simulations during the GA phase.

ACKNOWLEDGMENTS

This project was provided with computer and storage resources by GENCI at TGCC thanks to the grant 20XX-

AD010517004 on the supercomputer Joliot Curie's the ROME partition.

REFERENCES

[1] R. Geller, K. S. Golovanivsky, and G. Melin, "Ecripac: a new concept for the production and acceleration to very high energies of multiply charged ions using an ecr plasma", in *Proc. of the 10th international workshop on ECR ion sources*, pp. 449–451, 1991. https://www.osti.gov/biblio/6063139

[2] A. Cernuschi, T. Thuillier, and L. Garrigues, "Theoretical study of the electron cyclotron resonance ion plasma accelerator concept", *Physical Review E*, vol. 113, no. 4, p. 045211, 2026. doi:10.1103/5hk4-3md2

[3] A. Cernuschi, T. Thuillier, and L. Garrigues, "Milestone toward an electron cyclotron resonance ion plasma accelerator demonstrator", *Physical Review E*, vol. 113, no. 4, p. L043202, 2026. doi:10.1103/xfhl-nxgx

[4] R. Geller, *Electron cyclotron resonance ion source and ecr plasmas*. New York, USA: Routledge, 1996. doi:10.1201/9780203758663

[5] K. S. Golovanivsky, "The gyrac: a proposed gyro-resonant accelerator of electrons", *IEEE Transactions on Plasma Science*, vol. 10, no. 2, pp. 120–129, 1982. doi:10.1109/TPS.1982.4316150

[6] K. S. Golovanivsky, "The gyromagnetic autoresonance", *IEEE Transactions on Plasma Science*, vol. 11, no. 1, pp. 28–35, 1983. doi:10.1109/TPS.1983.4316213

[7] R. Bardet, T. Consoli, and R. Geller, "Physical mechanism of ion entrainment by the electron space charge in acceleration by the gradients of static magnetic and of electromagnetic fields", *Nuclear Fusion*, vol. 5, no. 1, pp. 7–16, 1965. doi:10.1088/0029-5515/5/1/002

[8] C. Birdsall and A. B. Langdon, *Plasma physics via computer simulation*. Boca Raton, USA: CRC Press, 1991. doi:10.1201/9781315275048

[9] Los Alamos National Laboratory, "Reference manual for the poisson/superfish group of codes", Los Alamos National Laboratory, NM, United States, Rep., 1987. doi:10.2172/10140827

[10] COMSOL Multiphysics, www.comsol.com

[11] V. V. Andreev, A. A. Novitskiy, A. M. Umnov, and D. V. Chuprov, "A pulse-periodic gyroresonant plasma accelerator", *Instruments and Experimental Techniques*, vol. 55, no. 3, pp. 301–312, 2012. doi:10.1134/S0020441212020121

[12] V. V. Andreev, D. V. Chuprov, V. I. Ilgisonis, A. A. Novitsky, and A. M. Umnov, "Gyromagnetic autoresonance plasma bunches in a magnetic mirror", *Physics of Plasmas*, vol. 24, no. 9, p. 093518, 2017. doi:10.1063/1.4986009

[13] V. V. Andreev, A. A. Novitsky, M. A. Korneeva, and A. M. Umnov, "Study of the development of relativistic plasma bunches in a long mirror trap by optical and x-ray imaging and numerical simulations", *Plasma Physics Reports*, vol. 43, no. 11, pp. 1114–1118, 2017. doi:10.1134/S1063780X17110010

[14] V. V. Andreev, V. I. Ilgisonis, A. A. Novitsky, and A. M. Umnov, "Generation of plasma bunches under conditions of gyromagnetic autoresonance in a long magnetic mirror machine: computational experiment", *Plasma Physics Reports*, vol. 46, no. 8, pp. 756–764, 2020. doi:10.1134/S1063780X20080012

[15] J. D. Jackson, "Classical electrodynamics", in *Encyclopedia of Applied Physics*. New York, NY, United States: John Wiley & Sons, Ltd, 2003. doi:10.1002/3527600434.eap109

[16] AF. Lifschitz, X. Davoine, E. Lefebvre, J. Faure, C. Rechatin, and V. Malka, "Particle-in-cell modelling of laser–plasma interaction using fourier decomposition", *Journal of Computational Physics*, vol. 228, no. 5, pp. 1803–1814, 2009. doi:10.1016/j.jcp.2008.11.017

[17] J. Derouillat *et al.*, "Smilei : a collaborative, open-source, multi-purpose particle-in-cell code for plasma simulation", *Computer Physics Communications*, vol. 222, pp. 351–373, 2018. doi:10.1016/j.cpc.2017.09.024

[18] J.-L. Vay *et al.*, "BLAST-WarpX/warpx: 26.05", Zenodo, May 2026. doi:10.5281/zenodo.20150594